

Key words: *ESP system, nonlinear optimisation methods*

WITOLD GRZEGOŹEK^{)}, STANISŁAW WOJCIECH^{**)}*

TIME-DOMAIN OPTIMISATION OF BRAKING TORQUE FOR THE ESP SYSTEM

An application of nonlinear optimisation methods to the solution of optimal brake torques for the ESP system is presented. The plane model of a vehicle is worked out and then used in the optimisation process. Two tasks are considered; the first when the vehicle motion is disturbed by bumps and ruts, the second when the vehicle changes the lane. The results of numerical calculation are included.

1. Introduction

ESP systems are more and more commonly applied to vehicles [5], [6], [7], [12]. When the braking torques that are applied on particular vehicle wheels are properly selected, in extreme vehicle situations, the stability of vehicle motion can be maintained. The values of braking torques are calculated as a results of the comparison of the basic parameters characterising vehicle motion, such as yaw velocity and side slip angle, that have been measured and calculated in real time by a board computer on a simple vehicle model [2], [3], [8], [9], [12]. The task of the resulting braking torques is to minimise the discrepancy between the parameters that were measured and calculated. Due to the necessity of real-time calculation, the vehicle model applied is a very simplified model. The results that have been obtained so far confirm the suitability of the applied simplification. The evaluation whether the application of the braking torques ensured an optimal realisation of the given manoeuvre is still an open question. The optimisation of the choice of the values of braking forces for a particular manoeuvre and the optimisation criterion connected with it would make such an evaluation possible. In this work, two optimisation tasks were fulfilled. The first

^{*)} *Cracow University of Technology, Al. Jana Pawła II 37, 31-864 Cracow, Poland; E-mail: witek@mech.pk.edu.pl*

^{**)} *Automotive Research and Development Centre BOSMAL, ul. Sarni Stok 93, 43-300 Bielsko-Biała, Poland; E-mail: swojciech@pb.bielsko.pl*

relates to the best choice of braking forces, so the deviation from rectilinear vehicle motion disturbed by bumps and ruts is reduced to the minimum. The second task is connected with a vehicle lane change manoeuvre, and for this task the optimisation criterion is the smallest possible loss of kinetic energy by the vehicle when the motion direction becomes parallel to the original one, and the defined lateral displacement has been completed. The first of the tasks described is a problem that is not taken into account in the standard ESP system. On the other hand, the second task is one of the manoeuvres, which often cause dangerous situations in vehicle motion. The method that is described may be also used for other optional manoeuvres occurring on the road.

2. Vehicle model

A simple plane vehicle model was prepared for optimisation tasks. The changes of wheel vertical loads caused by longitudinal and lateral acceleration were included in this model. The quasistatic method was used for designation of vertical wheel loads.

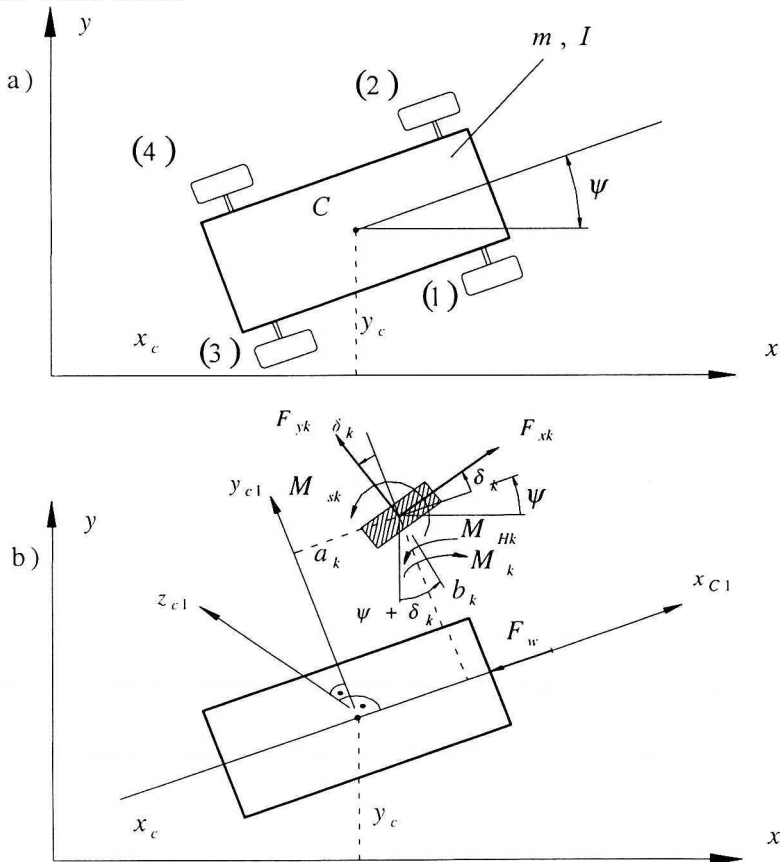


Fig. 1. Forces and moment acting on the vehicle: a) general view, b) forces and moment acting on the vehicle wheel k ($k=1,2,3,4$)

The equations of vehicle motion are as follows (Fig. 1):

$$\begin{aligned} m\ddot{x}_c &= \sum_1^4 F_{xk} \cos(\psi + \delta_k) - \sum_1^4 F_{yk} \sin(\psi + \delta_k) - F_w \cos \psi, \\ m\ddot{y}_c &= \sum_1^4 F_{xk} \sin(\psi + \delta_k) + \sum_1^4 F_{yk} \cos(\psi + \delta_k) - F_w \sin \psi, \end{aligned} \quad (2.1)$$

$$I\ddot{\psi} = \sum_1^4 \left\{ -b_k \left[F_{xk} \cos \delta_k - F_{yk} \sin \delta_k \right] + a_k \left[F_{xk} \sin \delta_k + F_{yk} \cos \delta_k \right] \right\} + \sum_1^4 M_{sk},$$

The equation of wheel motion is as follow

$$I_k \ddot{\phi}_k = M_k - M_{Hk} - F_{xk} \cdot r_{dk} + F_{zk} \cdot f'_k, \quad (k=1,2,3,4). \quad (2.2)$$

The vertical component of road force acting on the wheel is expressed as

$$N_k = -c'_k \Delta_k \quad (2.3)$$

- where: m – mass of a vehicle,
 I – moment of vehicle inertia,
 I_k – moment of wheel inertia,
 c'_k – reduced stiffness of suspension and tire,
 Δ_k – the sum of suspension and tire deflection,
 ψ – yaw angle,
 δ_k – wheel steering angle,
 F_{xk}, F_{yk}, F_{zk} – force components occurring at wheel- road point,
 F_w – wind force,
 M_{sk} – self aligning moment,
 M_k – driving torque,
 M_{Hk} – braking torque,
 r_{dk} – wheel radius,
 f'_k – equivalent coefficient of rolling resistance.

The longitudinal and lateral forces and self-aligning moments are expressed as:

$$\begin{aligned} F_{xk} &= \vartheta_k \cdot N_k, \\ F_{yk} &= \beta_k \cdot N_k, \end{aligned} \quad (2.4)$$

$$M_{sk} = \gamma_{xk} \cdot F_{xk} + \gamma_{yk} \cdot F_{yk} + \gamma_{k0} (F_{xk} \cdot F_{yk}) = \gamma_{k0} + \gamma_k \cdot N_k,$$

where: $\vartheta_k, \beta_k, \gamma_{k0}, \gamma_k$ are coefficients of tire model [4].

Thus the equations (2.1) we can express:

$$\begin{aligned} m\ddot{x}_c &= \sum_1^4 \vartheta_k \cdot c_{\psi k} \cdot N_k - \sum_1^4 \beta_k \cdot s_{\psi k} \cdot N_k - F_w \cdot c_{\psi}, \\ m\ddot{y}_c &= \sum_1^4 \vartheta_k \cdot s_{\psi k} \cdot N_k + \sum_1^4 \beta_k \cdot c_{\psi k} \cdot N_k - F_w \cdot s_{\psi}, \end{aligned} \quad (2.5)$$

$$\begin{aligned} I\ddot{\psi} &= \sum_1^4 \left\{ -b_k \left[\vartheta_k \cdot c_{\delta k} \cdot N_k - \beta_k \cdot s_{\delta k} \cdot N_k \right] + \right. \\ &\quad \left. + a_k \left[\vartheta_k \cdot s_{\delta k} \cdot N_k + \beta_k \cdot c_{\delta k} \cdot N_k \right] + \gamma_k \cdot N_k + \gamma_{k0} \right\}, \end{aligned}$$

or in equivalent form:

$$\begin{aligned} m\ddot{x}_c &= \sum_1^4 a_{xk} \cdot N_k + a_{x0}, \\ m\ddot{y}_c &= \sum_1^4 a_{yk} \cdot N_k + a_{y0}, \\ I\ddot{\Psi} &= \sum_1^4 a_{Mk} \cdot N_k + a_{M0}, \end{aligned} \quad (2.6)$$

where:

$$\begin{aligned} a_{x0} &= -F_w \cdot c_\psi, & a_{xk} &= \vartheta_k \cdot c_{\psi k} - \beta_k \cdot s_{\psi k}, \\ a_{y0} &= -F_w \cdot s_\psi, & a_{yk} &= \vartheta_k \cdot s_{\psi k} + \beta_k \cdot c_{\psi k}, \\ a_{M0} &= \sum_1^4 \gamma_{k0}, & a_{Mk} &= \gamma_k - b_k [\vartheta_k \cdot c_{\delta k} - \beta_k \cdot s_{\delta k}] + a_k [\vartheta_k \cdot s_{\delta k} + \beta_k \cdot c_{\delta k}], \\ s_\psi &= \sin \psi, & c_\psi &= \cos \psi, \\ s_{\psi k} &= \sin(\psi + \delta_k), & c_{\psi k} &= \cos(\psi + \delta_k), \\ s_{\delta k} &= \sin \delta_k, & c_{\delta k} &= \cos \delta_k, \\ \gamma_k &= \vartheta_k \cdot \gamma_{xk} + \beta_k \cdot \gamma_{yk}, \\ \gamma_{k0} &= \gamma_{k0} (F_{xk} \cdot F_{yk}). \end{aligned}$$

The self-aligning moment has the values calculated in the previous time step during integrating the equations.

In order to designate the values of vertical wheel loads, three equilibrium equations are applied. These have not been previously used for formulating the equation of motion.

$$\sum P_{iz'} = 0, \quad \sum M_{ix'} = 0, \quad \sum M_{iy'} = 0, \quad (2.7)$$

Linear and angular displacement of vehicle are presented in Fig. 2.

Assuming that roll and pitch angles are small, the coordinates of point A_k can be defined as

$$\mathbf{r}'_k = \begin{bmatrix} 1 & 0 & \theta & 0 \\ 0 & 1 & -\varphi & 0 \\ -\theta & \varphi & 1 & \Delta \\ 0 & 0 & 0 & 1 \end{bmatrix} \begin{bmatrix} a_k \\ b_k \\ 0 \\ 1 \end{bmatrix}. \quad (2.8)$$

Thus we obtain:

$$N_k = -c_k \cdot \Delta_k = -c_k [-\theta \cdot a_k + \varphi \cdot b_k + \Delta] \quad (2.9)$$

where: φ – roll angle,

θ – pitch angle,

Δ – vertical displacement of mass centre.

The resultant inertial force acting on the mass centre in system $\{c\}$ consists of the following components:

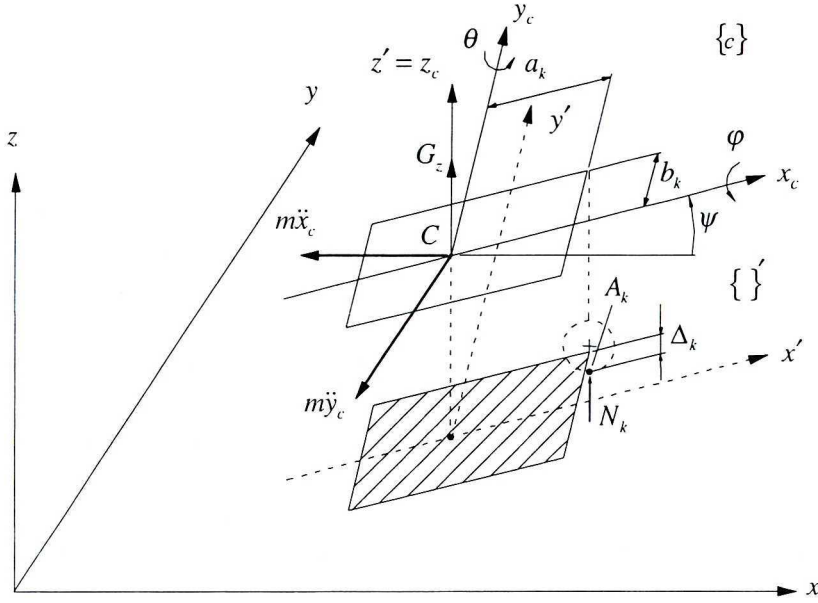


Fig. 2. Linear and angular displacement of the vehicle

$$\begin{aligned}
 P_{x_c} &= -m \cdot \ddot{x}_c \cdot c_\psi - m \cdot \ddot{y}_c \cdot s_\psi, \\
 P_{y_c} &= +m \cdot \ddot{x}_c \cdot s_\psi - m \cdot \ddot{y}_c \cdot c_\psi, \\
 P_{z_c} &= G_z,
 \end{aligned} \tag{2.10}$$

where: $s_\psi = \sin \psi$, $c_\psi = \cos \psi$.

When the equilibrium equations (2.7) are used we obtained:

$$\begin{aligned}
 \sum P_{iz'} &= \sum_1^4 N_k + P_{z_c} = 0, \\
 \sum M_{ix'} &= \sum_1^4 N_k \cdot b_k - P_{y_c} \cdot h = 0, \\
 \sum M_{iy'} &= -\sum_1^4 N_k \cdot a_k + P_{x_c} \cdot h = 0,
 \end{aligned} \tag{2.11}$$

where: h – height of mass centre.

We can present the result of the solution of the system equations (2.11) as:

$$\begin{aligned}
 \theta &= A_\theta + B_\theta \cdot \ddot{x}_c + C_\theta \cdot \ddot{y}_c, \\
 \varphi &= A_\varphi + B_\varphi \cdot \ddot{x}_c + C_\varphi \cdot \ddot{y}_c, \\
 \Delta &= A_\Delta + B_\Delta \cdot \ddot{x}_c + C_\Delta \cdot \ddot{y}_c,
 \end{aligned} \tag{2.12}$$

where the coefficients $A_\theta, B_\theta, C_\theta, A_\varphi, B_\varphi, C_\varphi, A_\Delta, B_\Delta, C_\Delta$ are described in [4].

After modification discussed in [4], we get the equations of motion in the form of:

$$\begin{aligned}
m\ddot{x}_c &= \sum_1^4 a_{xk} \left[N_{k0} + N_{kx} \cdot \ddot{x}_c + N_{ky} \cdot \ddot{y}_c \right] + a_{x0}, \\
m\ddot{y}_c &= \sum_1^4 a_{yk} \left[N_{k0} + N_{kx} \cdot \ddot{x}_c + N_{ky} \cdot \ddot{y}_c \right] + a_{y0}, \\
I\ddot{\psi} &= \sum_1^4 a_{Mk} \left[N_{k0} + N_{kx} \cdot \ddot{x}_c + N_{ky} \cdot \ddot{y}_c \right] + a_{M0},
\end{aligned} \tag{2.13}$$

where: $N_{k0} = -\dot{c}_k \cdot a_k \cdot A_\theta + \dot{c}_k \cdot b_k \cdot A_\phi + \dot{c}_k \cdot A_\Delta,$

$$N_{kx} = -\dot{c}_k \cdot a_k \cdot B_\theta + \dot{c}_k \cdot b_k \cdot B_\phi + \dot{c}_k \cdot B_\Delta,$$

$$N_{ky} = -\dot{c}_k \cdot a_k \cdot C_\theta + \dot{c}_k \cdot b_k \cdot C_\phi + \dot{c}_k \cdot C_\Delta.$$

The solutions of equations (2.13) are:

$$\begin{aligned}
\ddot{x}_c &= \frac{1}{w_m} [F_1 \cdot m_{22} - F_2 \cdot m_{12}], \\
\ddot{y}_c &= \frac{1}{w_m} [-F_1 \cdot m_{21} - F_2 \cdot m_{11}], \\
\ddot{\psi} &= \frac{1}{I} [F_3 - m_{31} \cdot \ddot{x}_c - m_{32} \cdot \ddot{y}_c],
\end{aligned} \tag{2.14}$$

where: $F_1 = m_{11} \cdot \ddot{x}_c + m_{12} \cdot \ddot{y}_c,$

$$F_2 = m_{21} \cdot \ddot{x}_c + m_{22} \cdot \ddot{y}_c,$$

$$F_3 = m_{31} \cdot \ddot{x}_c + m_{32} \cdot \ddot{y}_c + I\ddot{\psi}.$$

The coefficients $m_{11}, m_{12}, m_{21}, m_{22}, m_{31}, m_{32}$ are designated in [4].

The use of these equations makes it possible to diminish the time of integration, as it is not necessary to designate the values of the second derivatives of x, y, ψ by solving the linear algebraic equation system at each step of integration.

The Dugoff [1] tire model modified by Uffelmann was applied.

3. Formulation of optimisation tasks

The designation of the braking torque M_{Hi} that fulfills the required conditions and the minimisation of the objective function can be defined as the tasks of dynamic optimisation in the following forms:

I.1. find the minimum of the functional

$$F(t, q, \dot{q}, M_{H1}, M_{H2}), \tag{3.1}$$

I.2 ensure that the limiting conditions are fulfilled

$$g_p(t, q, \dot{q}, M_{H1}, M_{H2}) \leq 0 \quad \text{dla} \quad p = 1, \dots, n_a, \tag{3.2}$$

$$h_p(t, q, \dot{q}, M_{H1}, M_{H2}) = 0 \quad \text{dla} \quad p = 1, \dots, n_b, \tag{3.3}$$

I.3. ensure that the generalised coordinates and velocities fulfill the differential equations and the initial condition

$$A\ddot{q} = F(t, q, \dot{q}, M_{H1}, M_{H2}), \tag{3.4}$$

$$q|_{t=t_0} = q_0, \tag{3.5}$$

$$\dot{q}|_{t=t_0} = \dot{q}_1, \tag{3.6}$$

where q is the vector of generalized coordinates.

The task formulated in this way can be considered as a classical nonlinear optimisation task. If we assume that vector components are the decisive variables[10]:

$$M_1 = [M_{1,1}, M_{1,2}, \dots, M_{1,n_1-1}]^T, \tag{3.7}$$

$$M_2 = [M_{2,1}, M_{2,2}, \dots, M_{2,n_2-1}]^T, \tag{3.8}$$

where: $M_{i,j} = M_{Hi}(t_j)$; $i = 1, 2$; $j = 1, \dots, n$,

and torques are approximated by the spline function of the third order, then the task of dynamic optimisation (3.1), (3.2), (3.3) is reduced to the solution of the task of nonlinear optimisation as follows:

II 1. find the minimum of the functional

$$F(t, q, \dot{q}, M), \tag{3.9}$$

II 2. ensure that the limiting conditions such as:

$$g_p(t, q, \dot{q}, M) \leq 0 \quad \text{dla} \quad p = 1, \dots, n_a, \tag{3.10}$$

$$h_p(t, q, \dot{q}, M) = 0 \quad \text{dla} \quad p = 1, \dots, n_b, \tag{3.11}$$

are fulfilled.

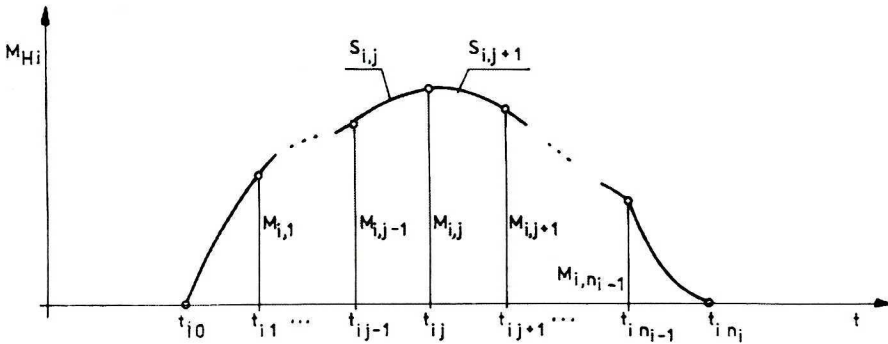


Fig. 3. The course of braking torques for optimisation tasks

II 3. ensure that q, \dot{q}, M fulfill the differential equation:

$$A\ddot{q} = F(t, q, \dot{q}, M), \tag{3.12}$$

and initial conditions:

$$q|_{t=t_0} = q_0, \tag{3.13}$$

$$\dot{q}|_{t=t_0} = \dot{q}_1, \tag{3.14}$$

where

$$M = \begin{bmatrix} M_{H1} \\ M_{H2} \end{bmatrix} = [M_{1,1}, \dots, M_{1,n1}, M_{2,1}, \dots, M_{2,n2}]^T.$$

This task (3.9), (3.10), (3.11) is a classical task of nonlinear optimisation with limits. However, the essential element of the second task is the fact that vector coordinates q, \dot{q} must be the solution of the initial task (3.12), (3.13), (3.14). For each combination of the components of the decisive variables in vector M , the equation (3.12) should be integrated in order to calculate vector component q and \dot{q} . In addition, the value of the functional (3.9) and the values of the function of border conditions g_p, h_p must also be calculated. In other words, the differential equation (3.12) should be integrated at each step of optimisation. That is why the problem of numerical effectiveness of models describing the dynamic system is getting more and more important. In this work, the method of Nadler–Made [10] was used for solving the optimisation task and the method of penalty function was used to solve the task with limits.

The formulated algorithm was used for solving the two tasks described below.

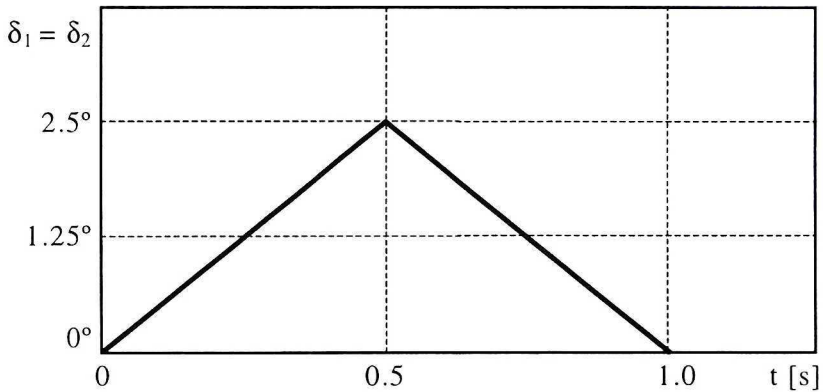


Fig. 4. Front wheel steering angle

Task I.

The vehicle motion is rectilinear. The driver is not going to change the motion direction. The initial velocity of the vehicle is 16,67 m/s. and the steering angle that is presented in Fig. 4 are assumed. The braking torque acting on the wheel should be chosen so that the functional

$$F = \frac{1}{t_k} \int_0^{t_k} \dot{\psi}^2 dt, \quad (3.15)$$

can be minimised.

That means that generation of minimal deviation of vehicle track from the straight line is possible. It was assumed that braking torque should meet the following condition

$$0 \leq M_{1,j} \leq 1300 Nm \quad (j = 1, \dots, n_i = 5) \quad (3.16)$$

to ensure that the wheel will not be locked.

The steering angle may be caused by bumps or ruts on the road. Simulation was carried out for a friction coefficient of 0.6. Figure 5 presents the course of braking torque on the outer wheel that is the result of optimisation. The value of acting torque did not reach the assumed limit and that is the reason why the braking wheel was not locked. In Fig. 6, the course of lateral displacement of the vehicle with and without braking torque is shown. The application of the braking torque caused only a small deviation from the rectilinear track of the vehicle, whereas in the opposite case this deviation exceeded 2.4 m.

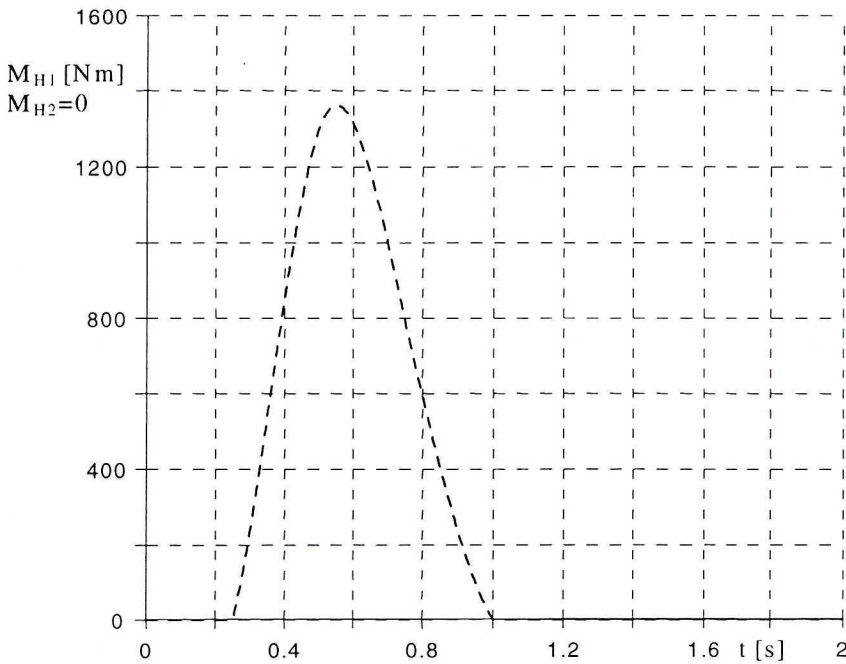


Fig. 5. The course of change in braking torques

The next Figure shows the course of parameters that characterise the vehicle motion when braking torque is acting. The values of side slip angle as well as the values of yaw velocity are minimal. The Figure also presents the limits $\dot{\psi}_{ref}$ for yaw velocity during turning of the front wheels calculated for the linear model of the vehicle.

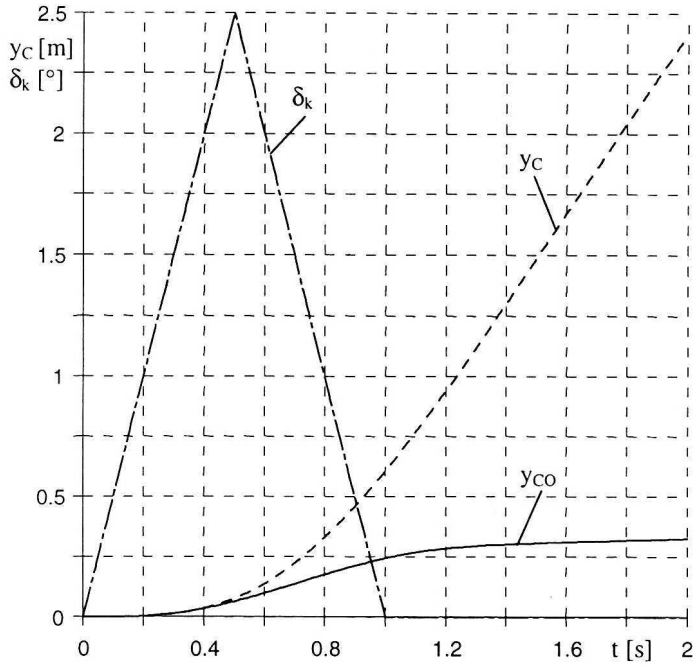


Fig. 6. The course of steering angle and vehicle track with (y_{co}) and without braking

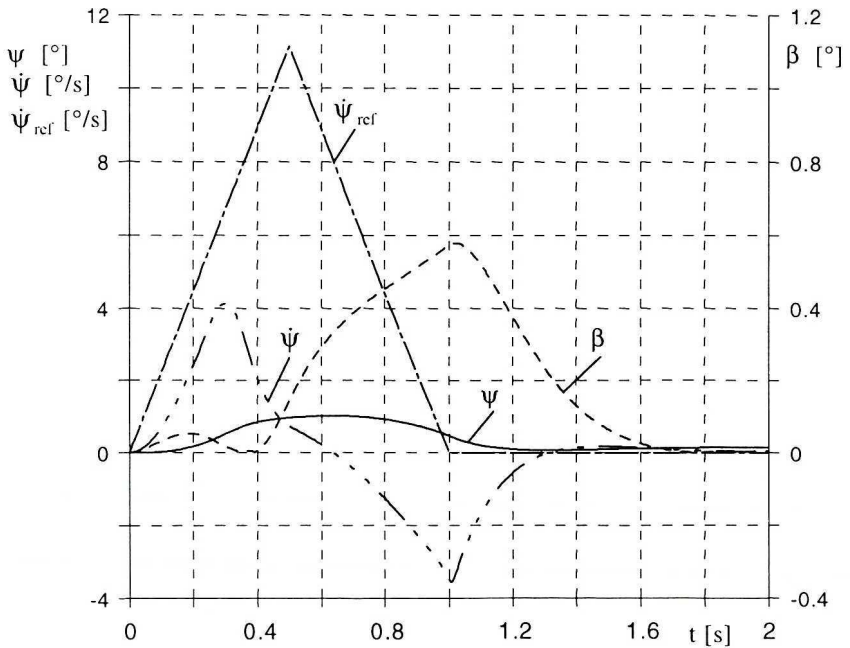


Fig. 7. The course of yaw velocity $\dot{\psi}$, side slip angle β , yaw angle ψ and limits

Task 2.

Assuming that steering angles had the courses presented in Figure 8, one should choose the torques M_{H1} , M_{H2} , so that the vehicle changes the lane, and at the end of the manoeuvre the vehicle should move in parallel to the initial track. The assumed steering angles correspond to the manoeuvre of changing the lane similarly to overtaking. The conditions limiting the M_{H1} , M_{H2} had the form of inequalities

$$0 \leq M_{i,j} \leq 1200 \text{ Nm} . \quad (3.17)$$

The possibility of wheel locking was not accepted.

The following limit [9], [12] for yaw velocity was assumed

$$|\dot{\psi}_{ref}| \leq \min \left\{ \left| \frac{v'_x \cdot \delta_k}{l \left(1 + \left(\frac{v'_x}{v_{char}} \right)^2 \right)} \right|, \frac{\mu_0 \cdot g}{v'_x} \right\}, \quad (3.18)$$

where: v'_x – longitudinal velocity of vehicle,

δ_k – steering angle,

l – wheel base,

v_{char} – characteristic velocity,

μ_0 – coefficient of friction,

g – gravity acceleration.

The first element of the right side of equation depends on the steering angle. That is why the condition for yaw velocity is checked when the yaw velocity exceeds a certain minimum value, that is when $|\dot{\psi}| \geq \dot{\psi}_{min}$.

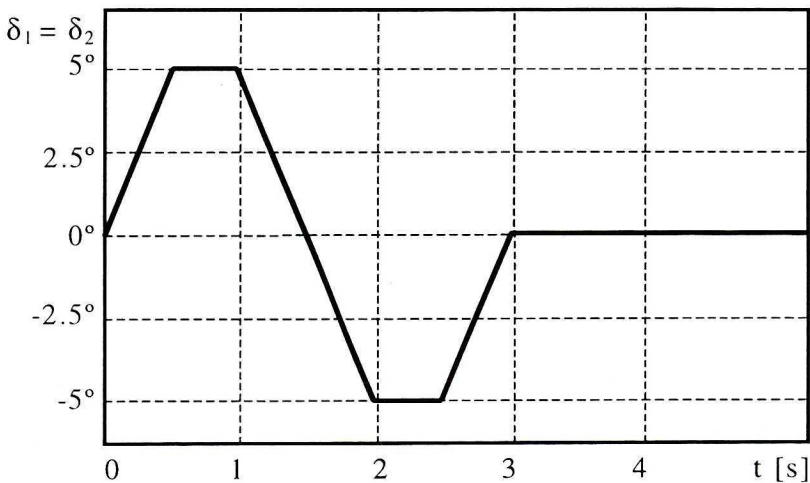


Fig. 8. Front wheel steering angle

For this task, the longitudinal velocity 16.67 m/s as well as minimum yaw velocity that equals $\dot{\psi}_{\min} = 0,151/s$ were taken into account. Moreover, it was assumed that the side slip angle should [7], [9] fulfill the condition:

$$|\beta| = \left| \frac{v_y}{v_x} \right| \leq 3 . \quad (3.19)$$

To make the longitudinal velocity vectors parallel at the beginning and at end of the manoeuvre, one assumed that at the end of manoeuvres the following condition should be fulfilled

$$|\psi|_{t=t_f} \leq \varepsilon_{\psi} \quad (\varepsilon_{\psi} = 0.01), \quad (3.20)$$

and, in addition, the maximum lateral displacement should meet the following condition $5 \text{ m} \leq y_{co} \leq 6 \text{ m}$.

The objective of optimisation is to select braking torques, so that the previous conditions are fulfilled and the following functional takes minimum value

$$F = \frac{1}{t_k} \int_0^{t_k} [v_0 - v]^2 dt , \quad (3.21)$$

where: v_0 – nominal velocity,

v – actual velocity,

that is the smallest possible loss of vehicle kinetic energy. Fig. 9 presents the results of this task when the friction coefficient equals 0.6. The values of the braking torques in the first cycle of the steering angle do not reach the assumed limit. Fig. 10 shows the lateral displacement of the vehicle when the runs of

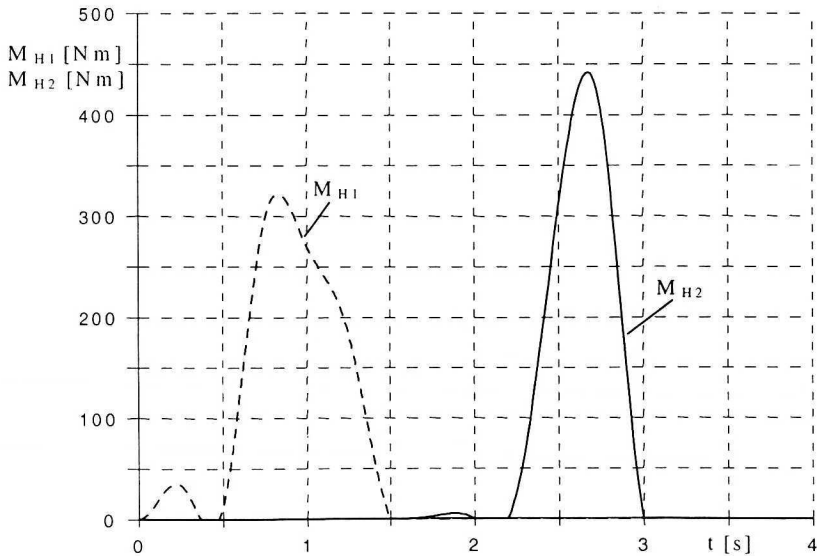


Fig. 9. The course of change in braking torques

braking torques M_{H1} , M_{H2} are as in Fig. 9, and the vehicle displacement such as for braking torques equal zero. There is a great difference between lateral displacement values. The application of braking torques made it possible to keep the displacement within the assumed limit.

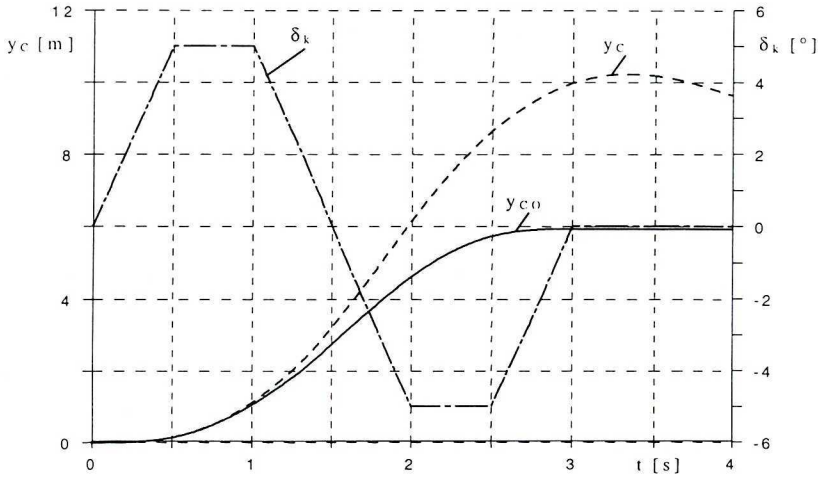


Fig. 10. The course of steering angle and vehicle track with(y_{c0}) and without braking

Figure 11 shows the course of parameters describing the vehicle motion and limits for yaw velocity defined when the brakes are used. Yaw velocity as well as side slip angle are within the assumed limits.

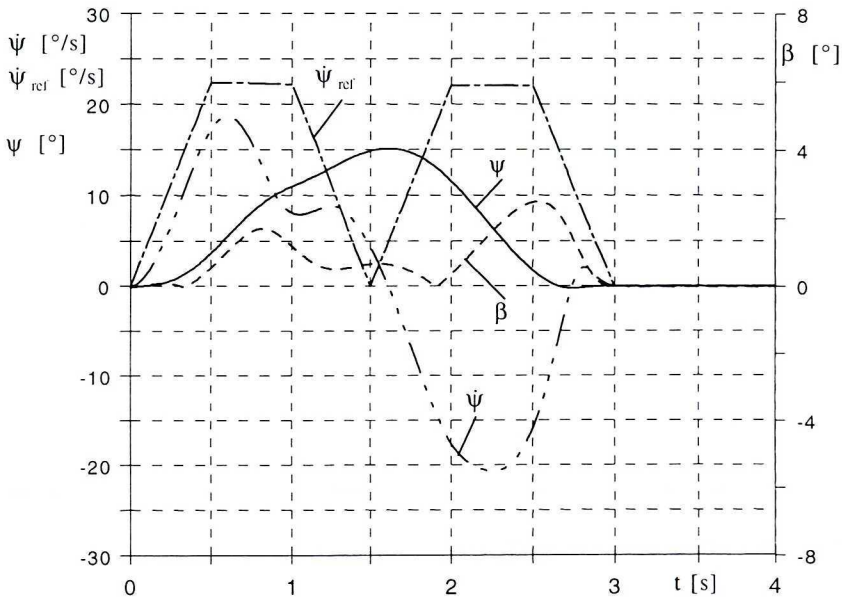


Fig. 11. The course of yaw velocity ψ , side slip angle β , yaw angle ψ and limits

4. Final remarks

The solution of this task, performed as an example of dynamic optimisation, requires several minutes of PC computer work. It is obvious that the method presented here cannot be used in controlling the vehicle motion in real time. However, this method can be used in design and research work. After experimental verification of the simple vehicle model, this method makes it possible to formulate and solve the complex optimisation tasks by using numerical methods without the necessity of making or modernising the real brake control system each time.

It is possible to carry out the simulation covering optimisation that reflects certain typical road situations. The results of this simulation, in the form of a certain number of patterns, could be stored in the computer memory that controls the system. On the other hand, the measurements made during real motion could be used to correct these solution patterns.

This method can be used for evaluating the operation of the real ESP.

Manuscript received by Editorial Board, November 05, 2001;
final version, January 31, 2002.

REFERENCES

- [1] Dugoff H., Fancher P.S., Segel L.: An Analysis of Tire Traction Properties and Their Influence on Vehicle Dynamics Performance. SAE Technical Paper 700377.
- [2] Fennel H.: Modulare Strukturen für das Elektronische Stabilitätsprogramm ESP. System Partners 99, ATZ 101 (1999), pp. 12÷18, Sonderausgabe ATZ / MTZ.
- [3] Furukawa Y., Abe M., Advanced Chassis Control Systems for Vehicle Handling and Active Safety. Vehicle System Dynamics, v. 28 (1997), pp. 59÷86.
- [4] Grzeźoźek W., Adamski W.: Model i program komputerowy do analizy dynamiki i stateczności ruchu pojazdu. Zeszyty Naukowe OBR „Bosmal” Bielsko–Biała, z. 11, 2000, pp. 11÷35.
- [5] Matsumoto S., Yamaguchi H., Inoue H., Yasuno Y.: Braking Force Distribution Control for Improvement Vehicle Dynamics. SAE Paper 923079.
- [6] Müller A., Achenbach W., Schindler E., Wohland T., Mohn F.: Das neue Fahrsicherheitssystem Electronic Stability Program von Mercedes Benz. ATZ 96 (1994), h. 11, pp. 656÷670.
- [7] Shibahata Y., Shimada K., Tomari T.: Improvement of Vehicle Maneuverability by Direct Yaw Moment Control. Vehicle System Dynamics 22 (1993), pp. 465÷481.
- [8] Yamamoto M., Inagaki S., Kushiro I.: Improvement of Vehicle Stability in Critical Cornering by Active Brake Control. Toyota Technical Review, v.45, no 1,1995, pp. 64÷69.
- [9] Witte B.: Stabilisierung der Gierbewegung eines Kraftfahrzeuges in kritischen Fahrsituationen. Verkehrstechnik/Fahrzeugtechnik VDI, nr 254, Düsseldorf 1995.
- [10] Wit R.: Metody programowania nieliniowego. Minimalizacja funkcji gładkich. WNT Warszawa, 1986.

-
- [11] Wojciech S.: Dynamic Analysis of Manipulator with Consideration of Dry Friction. *Computer & Structures*, Vol. 57, No 6, 1995, pp. 1045+1050.
- [12] Van Zanten A, Erhardt R., Pfaff G.: Die –Fahrdynamikregelung von Bosch. *ATZ 96* (1994), h. 11, pp. 674+689.

Optymalizacja momentu hamującego w dziedzinie czasu dla systemu ESP

S t r e s z c z e n i e

Praca zawiera opis zastosowania nieliniowych metod optymalizacji dla rozwiązania problemu optymalnego doboru momentów hamujących dla potrzeb systemu ESP. Dla zastosowania optymalizacji opracowano płaski model pojazdu, tak aby zapewnić dużą efektywność numeryczną symulacji komputerowej. Rozważane były dwa zadania: pierwsze w którym prostoliniowy ruch pojazdu zakłócony był przez nierówności drogi, drugie w którym pojazd zmieniał pas ruchu. Zastosowanie w modelu pojazdu optymalnych wartości momentów hamujących pozwoliło na zachowanie stabilności ruchu pojazdu w rozważanych manewrach.